RESOLUTION ENHANCEMENT OF THERMAL IMAGES VIA MULTITEMPORAL FUSION OF ETHEROGENEOUS DATA

Rita Montone[1], Paolo Addesso[1], Riccardo Garella[1], Maurizio Longo[1], Rocco Restaino[1] and Gemine Vivone[2]

1. University of Salerno, Department of Information Engineering, Electrical Engineering and Applied Mathematics, Fisciano (SA), Italy; {rmontone, paddesso, longo, restaino}@unisa.it
2. North Atlantic Treaty Organization (NATO) Science and Technology Organization (STO) Centre for Maritime Research and Experimentation, 19126 La Spezia, Italy; vivone@cmre.nato.int

ABSTRACT

Remotely sensed thermal data are of major interest for a variety of environmental and agricultural applications, allowing for the continuous estimation of geophysical features over wide areas. However, the effective use of these techniques often requires images with both high spatial resolution (HSR) and high temporal rate (htr), which constitute conflicting requirements for a single sensor. A solution can be achieved through data fusion techniques that provide improved synthetic images by taking advantage of data collected by multiple sensors. In this perspective we investigate in this study a method for combining thermal image sequences with complementary features, evaluating several different approaches for completing this task. The paper reports the analysis of several approaches based on deterministic interpolation and fusion schemes, focusing on the integration of data collected by the recent VIIRS sensor with data provided by the SEVIRI and MODIS instruments.

KEYWORDS

Remote Sensing, Data Fusion, Brightness Temperature, Thermal Image Enhancement

INTRODUCTION

Thermal infrared satellite observations of the Earth's surface are key components in estimating the Land Surface Temperature (LST) that plays an important role for several applications such as forest fires monitoring, climate models and crop growth modeling. More specifically, the present study has been motivated by the IRRISAT project for sustainable irrigation (1) that requires an accurate estimation of the thermal inertia for monitoring the soil moisture (2).

High frequency of observation and high spatial resolution are desirable to accurately follow the evolution of LST. However, acquisitions from a single satellite are limited, due to physical constraints, in either spatial or temporal resolution. Indeed we have sensors placed on geostationary platforms (like SEVIRI), which produce almost continuously data (an image each 15 minutes), but with very poor spatial resolution (around 6 km) and sensors placed on polar satellites (like MODIS and VIIRS) that are characterized by a high spatial resolution (1 km and 375 m, respectively), but very low revisiting period (about 4 and 12 hours). In particular, the VIIRS instrument was launched in October 2011 as part of the Suomi National Polar-orbiting Partnership, and is referred to as the next-generation Earth observation instrument. It will be the primary source of systematic land remote sensing products until about 2022 and is expected to yield significant improvements with respect to its predecessors in terms of Earth observation quality.

In order to meet the typical applications' requirements, image fusion of data acquired by multiple sensors with complementary features has been suggested as a way of producing synthetic data with high spatial and temporal resolution at the same time (3). In this paper we examine several possible approach for interpolating the available data in order to obtain a set of homogeneous sequences and we test some combination rules aimed at fusing the interpolated sequences. More

in detail, we test a fusion architecture for the combination of SEVIRI data with both the MODIS and the VIIRS images, highlighting the improvements achievable by employing the images collected by the sensor mounted on the recent NPP satellite. The performances are assessed in a controlled scenario constructed by simulating the required thermal image sequences from a real SEVIRI sequence.
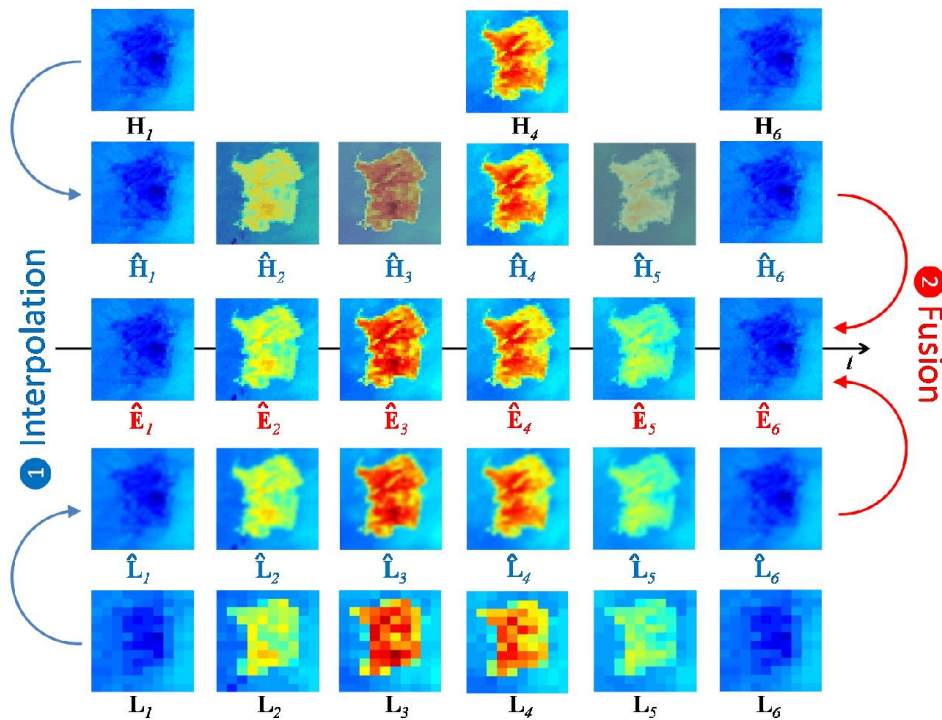
Figure 1: Timeline of the estimated quantities.

METHODS

The paper deals with procedures for constructing an estimate $\hat{E} = \{\hat{E}_k : k \in T_E\}$ of a high temporal rate and High Spatial Resolution (*htr/HSR*) image sequence $E = \{E_k : k \in T_E\}$ by employing deterministic interpolation and fusion rules. The algorithm entails two successive steps (see Figure 1): in the first one the available data are resized to the same spatial resolution and temporal rate of the target sequence through interpolation methods; the second step has the purpose of combining the resized sequences and exploits a deterministic fusion rule.

The first phase aims at reconstructing the missing information by exploiting spatial and temporal interpolation algorithms, under the implicit assumption that the high temporal rate and Low Spatial Resolution (*htr/LSR*) sequence $L = \{L_k : k \in T_L\}$ and the low temporal rate and High Spatial Resolution (*ltr/HSR*) sequence $H = \{H_k : k \in T_H\}$ are subsampled versions of the *htr/HSR* sequence E. However, while the spatial interpolation of the *htr/LSR* sequence consists in filling a regular grid, finer than the original (regular as well) one, with inferred new values, the temporal interpolation aims at reconstructing the temporal evolution of the pixels from a small set of (usually) non-uniformly spaced samples. In this work the latter procedure is simplified by treating each pixel independently, thus neglecting the spatial correlation, with the aim of applying one-dimensional interpolation algorithms. Spatial interpolation of images has been the subject of many papers in the technical literature (4,5), also with specific reference to image sharpening (6). As to the temporal interpolation of the *ltr/HSR* sequences, real cases are characterized by large nonuniform intervals

among available samples. Thus, in practice, an *optimal* interpolation scheme is hardly defined and the interpolation is commonly performed through heuristic blockwise procedures (7,8). After a detailed investigation of the different interpolation methods we selected the *cubic convolution kernels* (9) for the spatial interpolation and the *shape preserving Hermite polynomial* scheme (10) for the temporal interpolation.

A wide range of fusion methods can be found in the literature for completing the second step; actually, the combination of images acquired from different sensors requires some additional preprocessing procedures, since each sensor has its own characteristics, and the images also need to be geometrically corrected and co-registered. The pansharpening literature contains several approaches (11) that can be adapted to the fusion of thermal images to account for their peculiarities (12). The general scheme encompasses two distinct phases (13): 1) the extraction of details from an HSR image and 2) their injection into the time co-located *LSR* image. A successful fusion scheme that we employ in this paper is the *Amélioration de la Résolution Spatiale par Injection de Structures* (ARSIS) method: at each instant the enhanced image is obtained by preserving the whole information contained in the *LSR* image and in adding the details extracted from the HSR image through a multiresolution scheme. The latter was carried out through an undecimated wavelet decomposition employing the "à trous" algorithm.
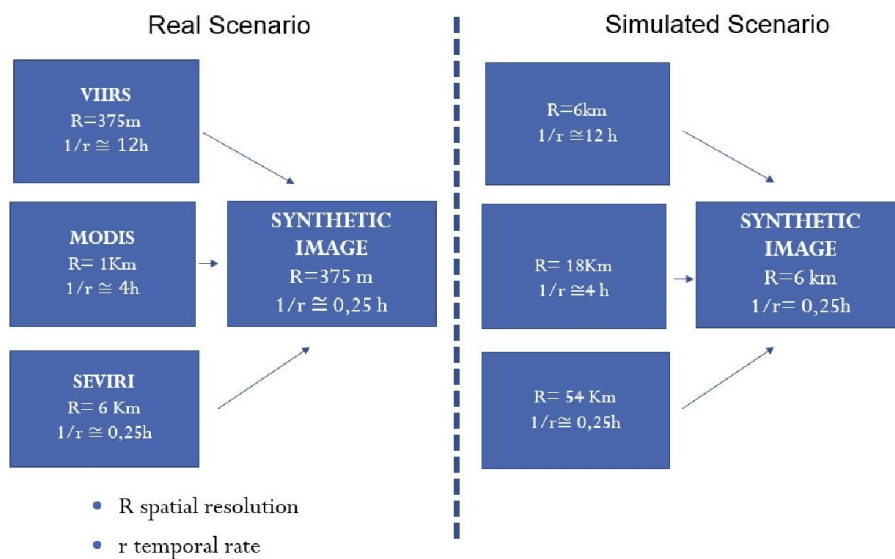
Figure 2: Assessment protocol.

EXPERIMENTAL RESULTS

The experiment is framed in a simulated scenario, constructed by starting from a single sequence of SEVIRI images (10.8IR channel). The image sequence has been acquired on the Iberian peninsula (latitude between 35.7° and 41.4° North, longitude between 4.1° and 9.8° West), on August 16, 2014. The original SEVIRI sequence plays the role of the *htr/HSR* sequence to be estimated (or Ground Truth) and the three sequence to fuse are simulated by reproducing the spatial resolution ratios among the SEVIRI, MODIS and VIIRS sensors, as illustrated in Figure 2.
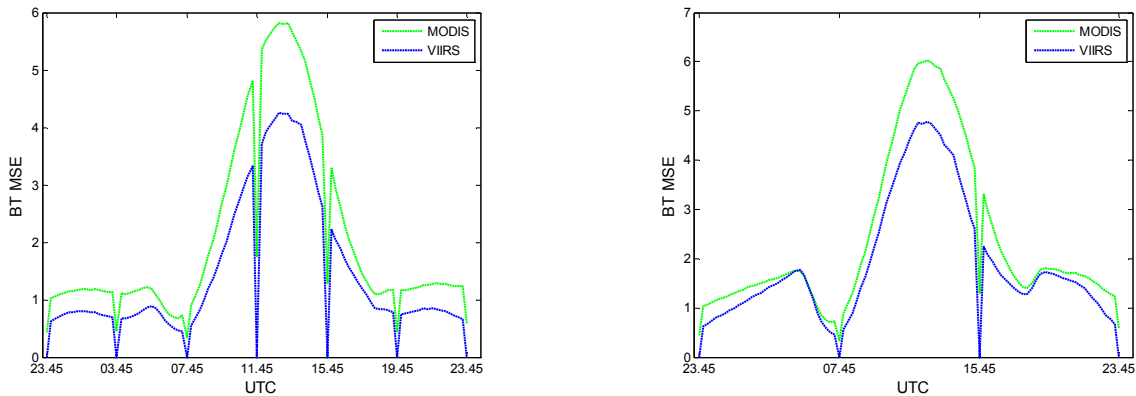
Figure 3: MSE vs. time of the estimated sequence obtained by employing the MODIS (upsampled to the VIIRS resolution) and the VIIRS data as ltr/HSR sequences: on the left ΔH=4 h, on the right ΔH=8 h.

AVERAGE MSE [K²]		
ΔH [h]	MODIS	VIIRS
4	2.081	1.416
8	2.364	1.862

Table 1: Average MSE of the estimated sequence obtained by employing the MODIS and the VIIRS data as ltr/HSR sequences.

We assess the performances in terms of Mean Square Error (MSE) that is the most widely used quality index for Brightness Temperatures. In particular, we firstly compare the ideal performances achievable by employing the sole MODIS sequence or the sole VIIRS sequence in conjunction with the SEVIRI sequence. More specifically, profiting from the perfectly controlled framework, we tested the algorithms with diverse intervals *ΔH* between the HSR images. The behaviour of the MSE during an observation day is reported in Figure 3, with reference to *ΔH={4,8}* h and reinforces the intuition that the improvements achievable by using a higher quality ltr/HSR are inversely related to *ΔH*. Table 1 reports the MSE values averaged over the whole day.

(a)   (b)
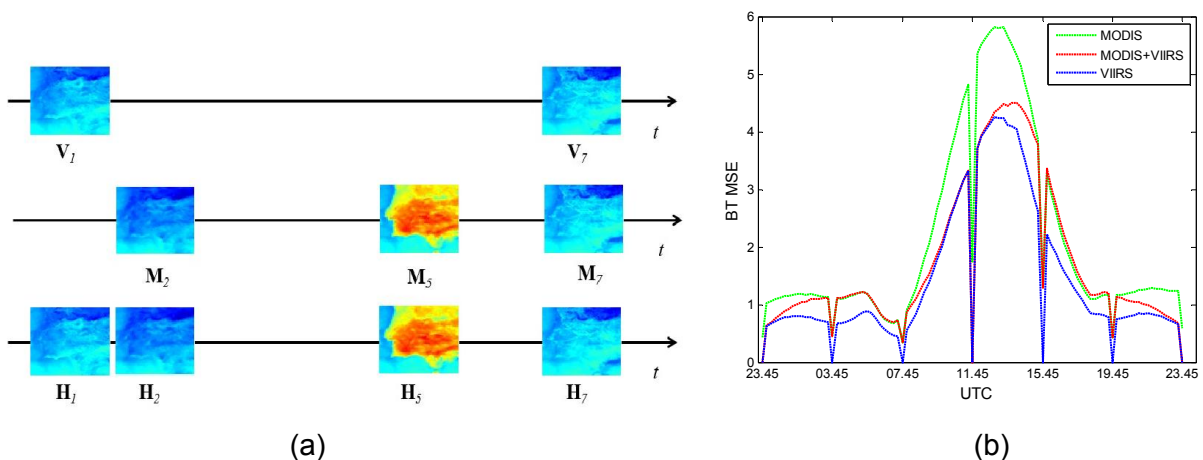
Figure 4: Two ltr/HSR image sequences are available: V denotes the VIIRS sequence, and M the MODIS sequence: (a) the construction of the ltr/HSR sequence; (b) MSE vs. time of the estimated sequence.

However, in the real practice the VIIRS data are scarcely available, since the revisit time is typically of the order of 12 hours. For that reason, we further design a test more similar to the real situation; namely, as depicted in Figure 4(a), we construct the *ltr/HSR* sequence H by joining the MODIS $M = \{M_k : k \in T_M\}$ and the VIIRS sequence $V = \{V_k : k \in T_V\}$. In particular, we use the VIIRS image if available, and a MODIS image, upsampled to the VIIRS resolution, otherwise. The MSE is shown in Figure 4(b) and evidences the valuable contribution entailed by the use of the three VIIRS image; indeed we achieved an average MSE equal to 2.081 K^2 by using the sole MODIS images and an average MSE 1.719 K^2 by using also the VIIRS images.

We finally note that the fused sequence S can also been used for feeding Bayesian smoothing algorithms that are able to exploit the correlation within images to produce an improved estimate (14). The results achievable by employing a Forward Kalman Filter, a Backward Information Filter (BIF) and a *Forward-Backward* Smoother (FBS) algorithm are shown in Figure 5 and the corresponding average values are reported in Table 2.
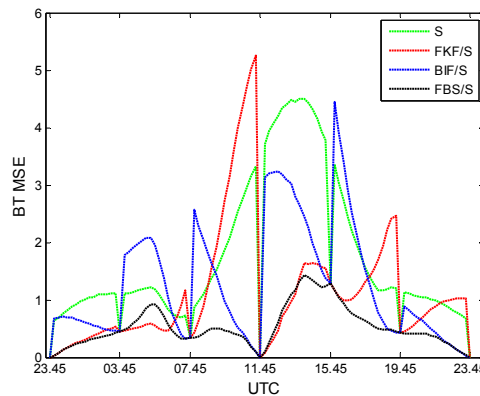
Figure 5: MSE vs. time of the estimated sequence by employing Bayesian sequential algorithms.

AVERAGE MSE [K^2]					
SCENARIO	ΔH [h]	S	FKF/S	BIF/S	FBS/S
MODIS+VIIRS	**4**	**1.719**	**1.115**	**1.273**	**0.524**

Table 2: Average MSE achieved by employing a FKF, a BIF and a FBS.

CONCLUSIONS

In this study we assessed an approach based on interpolation and sharpening techniques for enhancing the temporal and spatial resolution of thermal image sequences through the combination of multisensor data having complementary features.

We evaluated the performances of the proposed algorithms in a simulated scenario that allows to test the proposed methods in many different working setups. In particular we employed real acquisitions provided by the SEVIRI sensor for mimicking the characteristics of VIIRS, SEVIRI and MODIS sensors and assessed the improvements achievable by the use of the new sensor mounted on the NPP platform.

Further investigations will be devoted to the validation on real sequences; the new test will also include the preliminary detection of cloudy pixels (15,16): indeed in the presence of occlusion due to cloud masses also the *htr/LSR* image sequence should be spatially and temporally interpolated in order to replace the actual BT, reflected by the top of the clouds, with a fictitious BT, translated to the land surface level.

ACKNOWLEDGEMENTS

REFERENCES

1   IRRISAT Project, 2011. Pilotaggio dell'irrigazione a scala aziendale e consortile assistito da satellite. Available: http://www.irrisat.it

2   Maltese A, F Capodici, G Ciraolo, and G La Loggia, 2013. Map soil water content under sparse vegetation and changeable sky conditions: comparison of two thermal inertia approaches. Journal of Applied Remote Sensing, 7: 073548–1 – 073548–17.

3   Addesso P, R Conte, M Longo, R Restaino & G Vivone, 2012. A sequential Bayesian procedure for integrating heterogeneous remotely sensed data for irrigation management, Proc. SPIE Remote Sensing, 85310C-1-- 85310C-10.

4   Parker J A, R V Kenyon, D E Troxel, 1983. Comparison of interpolation methods for image resampling. IEEE Transaction on Medical Imaging, MI-2: 31–39.

5   Maeland E, 1988. On the comparison of interpolation methods. IEEE Transactions on Medical Imaging,7: 213-217.

6   B Aiazzi, S Baronti, M Selva & L Alparone, 2013. Bi-cubic interpolation for shift-free pan-sharpening, ISPRS Journal of Photogrammetry and Remote Sensing, 86: 65-76.

7   Marvasti F E Ed.,2001. Nonuniform Sampling, Theory and Practice (Kluwer Academic/Plenum), 924 pp.

8   Tuncer T E, 2007. Block-based methods for the reconstruction of finite-length signals from nonuniform samples. IEEE Transactions on Signal Processing, 55: 530-541.

9   Keys R 1981. Cubic convolution interpolation for digital image processing. IEEE Trans. Acoust., Speech, Signal Process. 29: 1153–1160.

10 Akima H 1970. A new method of interpolation and smooth curve fitting based on local procedures. J. ACM 17: 589–602.

11 Ha W, P H Gowda & T A Howell, 2013. A review of potential image fusion methods for remote sensing-based irrigation management: part II. Irrigation Science, 31:, 851–869.

12 Zhan W, Y Chen, J Zhou, J Li & W Liu, 2011. Sharpening thermal imageries: A generalized theoretical framework from an assimilation perspective. IEEE Transactions on Geoscience and Remote Sensing. 49: 773–789.

13 Vivone G, L Alparone, J Chanussot, M Dalla Mura, A Garzelli, G Licciardi, R Restaino, L Wald, 2015. A Critical Comparison Among Pansharpening IEEE Trans. Geosci. Remote Sens., 53: 2565-2586.

14 Fraser D & J Potter 1969. The optimum linear smoother as a combination of two optimum linear filters. IEEE Transactions on Automatic Control, 14: 387–390

15 P Addesso, R Conte, M Longo, R Restaino, G Vivone, 2012. MAP-MRF cloud detection based on PHD filtering, IEEE Journal of Selected Topics in Applied Earth Observations and Remote Sensing, 5: 919-929.

16 Vivone G, P Addesso, R Conte, M Longo, R Restaino, 2014. A Class of Cloud Detection Algorithms based on a MAP-MRF Approach in Space and Time, IEEE Transaction on Geoscience and Remote Sensing, 52: 5100-5115.